Journal of Materials Processing Technology
Article in Press, Corrected Proof

http://dx.doi.org/10.1016/j.jmatprotec.2008.02.060

Oxidation-induced strength behavior of Ti_3SiC_2

D. Sarkar, A. Padhiary, S.J. Cho and M.C. Chu

Department of Ceramic Engineering, National Institute of Technology, NIT-Rourkela, Rourkela 769008, Orissa, India

[b]Division of Advanced Technology, Korea Research Institute of Science and Standards, Yusong, Daejeon 305-600, Republic of Korea

Abstract

Oxidation behavior and subsequent mechanical properties of Ti_3SiC_2 were studied. The oxide scale has significant effect on strength and hardness, which is mainly attributed due to the mismatch of coefficient of thermal expansion (CTE) of substrate and oxide phases. The improved flexural strength (~650 MPa) could be noticed at 1000 °C; however, at elevated temperature the ductility of Ti_3SiC_2 was predominant and reduced the strength.

Keywords: Oxidation; Flexural Strength; Ti_3SiC_2

1. Introduction

Recently, Ti_3SiC_2 is identified as a new class of thermodynamically stable nanolaminate ductile ceramic exhibiting features of both metallic and ceramic materials (Barsoum and El-Raghy, 1996). Some of the key properties of Ti_3SiC_2 include excellent resistance to oxidation up to 1400 °C, high modulus (~320 GPa), high thermal shock resistance, relatively low hardness (4–5 GPa), high fracture toughness (7–9 MPa $m^{1/2}$) and good machinability (El-Raghy et al., 1999; Sarkar et al., 2006a,b). Additionally, room temperature compressive and three-point bending strengths of TiC containing Ti_3SiC_2 are 1120 and 350 MPa, respectively (Rudnik and Lis, 1997). The high temperature compressive strength behavior of Ti_3SiC_2 under vacuum exhibits interesting aspects. The shear fracture and fracture strength of Ti_3SiC_2 decrease monotonically from 935 MPa (25 °C) to 640 MPa (930 °C) (Zhang and Sun, 2005). Moreover, Ti_3SiC_2 is also a damage-tolerant material and has a brittle-to-ductile transition at 1200 °C (Radovic et al., 2000). Ti_3SiC_2 is one of the most potential materials for high temperature structural component though it starts oxidizing in air. In this context, Racault et al. (1994) pointed out that oxidation of Ti_3SiC_2 initiate at 400 °C with formation of TiO_2 (antase) film. The process of oxidation is activated above 1050 °C with the formation of rutile and cristobalite. Oo et al. (in press) illustrated that the oxidation of Ti_3SiC_2 starts at around 750 °C to form rutile (TiO_2), which reaches a maximum content of ~75 wt% at 1100 °C, where the oxide scale on Ti_3SiC_2 is stratified as an outer layer of TiO_2 and an inner layer of TiO_2 and SiO_2. The bending strength (~180 MPa) of the developed oxide scale is lower than that of Ti_3SiC_2 substrate (Bao et al., 2007). The observed variation of oxidation behavior could be due to the presence of second phase and processing parameters. Interestingly, the coefficient of thermal expansion (CTE) value of these oxide phases is different, which may govern the strengthening behavior through development of compressive residual stress on surface (Manoun et al., in press). In a recent work, alumina has been (~60%) strengthened and/or healed through adopting this phenomenon and showed moderate mechanical and tribological properties (Chu et al., 2005, in press; Sarkar et al., 2007a,b). Different schools are also engaged to study the effect of oxidation on strength behavior

* Corresponding author. Tel.: +91 661 2462207; fax: +91 661 2462999.
E-mail address: dsarkar@nitrkl.ac.in (D. Sarkar).

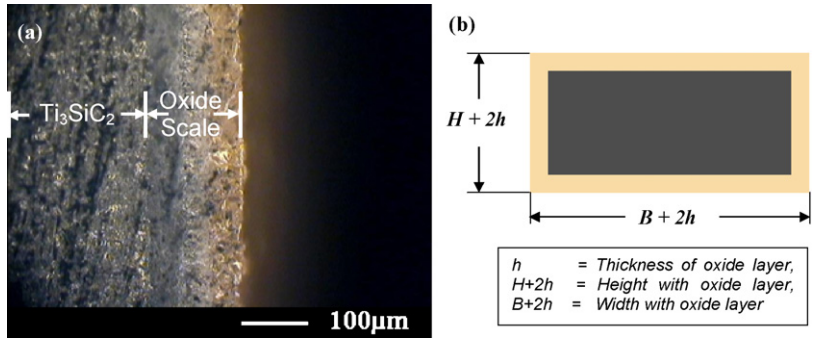

Fig. 1 – Optical microscopic image of cross-sectioned T_4 surface (a). Schematic of cross-sectioned surface of oxidized Ti_3SiC_2, where '*h*' is thickness of oxide scale, '*H*' and '*B*' are the height and width of unoxidized Ti_3SiC_2 surface, respectively (b). Typical dimension of as-received Ti_3SiC_2 specimen was 3 mm (height) × 4 mm (width) × 40 mm (length).

for different non-oxide ceramics like WC-Co and SiC (Casas et al., 2001; Chu et al., 2006). However, studies of the effect of oxidation on the mechanical properties of Ti_3SiC_2 are relatively scarce, and hence the prime objective of the present report is to optimize the oxidation temperature to improve the strength behavior of Ti_3SiC_2.

2. Experimental

Ti_3SiC_2 specimen was prepared through hot pressing method. Detail processing procedure could be found elsewhere (Sarkar et al., 2005, 2006a,b). Disks were then machined into flexural specimens of 3 mm × 4 mm × 40 mm and separately heat-treated at 700, 1000 and 1200 °C for 2 h in air and the samples were designated as T_2, T_3 and T_4, respectively; whereas original sample was denoted as T_1. Heating rate was 5 °C min^{-1} and cooling was done by turning off the electric power of the furnace. Specimens were placed on a holder in such a manner that width of the specimen was oriented along the perpendicular to the tensile stresses applied during the strength measurement. Subsequently, the oxidized samples were cut down by diamond saw along the cross-section and analyzed through optical microscope (ZEISS, Axiotech) and scanning electron microscopy (JEOL-JSM840) equipped with Energy Dispersive X-ray (EDX) spectroscopy. For SEM analysis, the oxide scale was coated with a thin film of Au. Phase analyses of oxidized surfaces were carried out using X-ray Diffraction (Cu, Kα, PHILIPS PW1830) technique. The specimens were also heated in a dilatometer (NETZSCH DIL402C) with heating and cooling rate of 5 °C min^{-1} using high grade quartz as reference up to 1200 °C. Flexural strength (Hounsfield H10 KS) of oxidized specimens was determined by standard 3-pt bending method in an instrument with 30 mm span and cross-head speed of 0.5 mm min^{-1}. The elastic modulus (*E*) of oxidized specimens was measured using an ultrasonic tester

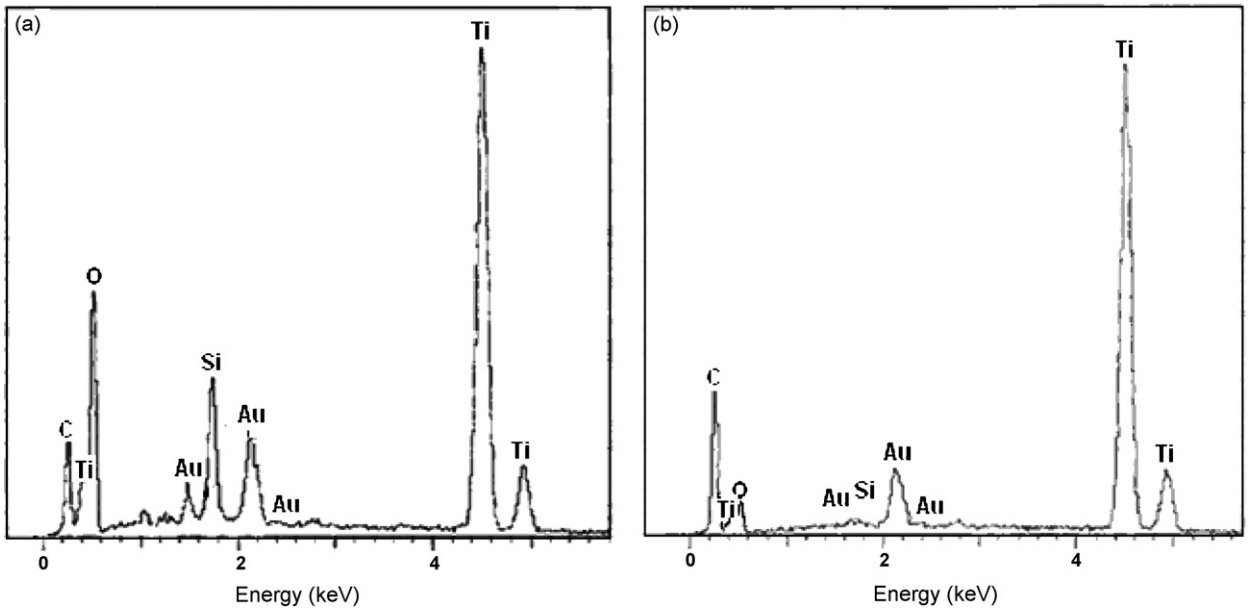

Fig. 2 – SEM-EDX analysis of inner layer (a) and outer layer (b) of cross-sectioned surface of T_4 specimen. Qualitative element analysis indicate the content of Si and O is higher in inner layer with compare to outer layer. The outer layer is mainly composed of TiO_2, whereas inner layer is mixture of TiO_2 and SiO_2.

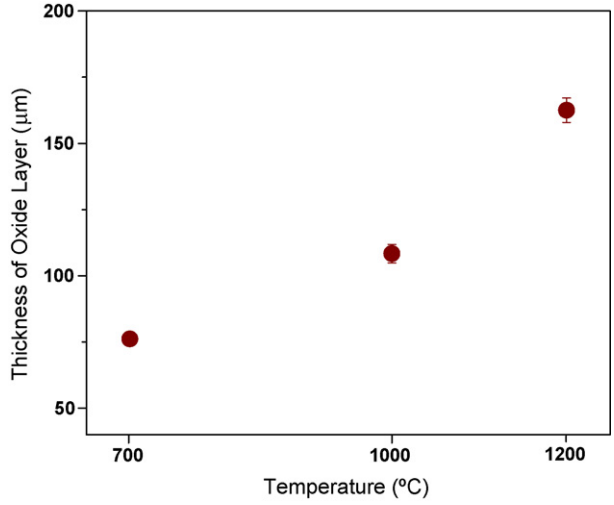

Fig. 3 – The thickness of oxide scale varies with respect to temperature. All the specimens are heat-treated for 2 h at corresponding peak temperatures.

employing the pulse-echo technique (Sarkar et al., 2007a,b). Prior to Vickers hardness determination at 98 N load, the specimens were polished down to mirror finish by diamond paste.

3. Results and discussion

Fig. 1(a) illustrates the optical microscopic image of cross-section of T_4. A significant color difference could be noticed across the outer to inner oxidized surface because of the presence of different oxide phases. To determine the fracture strength of oxide scale, a schematic view of cross-sectioned surface of oxidized Ti_3SiC_2 specimen with a constant oxide thickness of '*h*' mm is illustrated in Fig. 1(b), where width and height of the specimen are represented as '*B*' and '*H*', respectively. Fig. 2 shows the EDX analysis along the cross-section

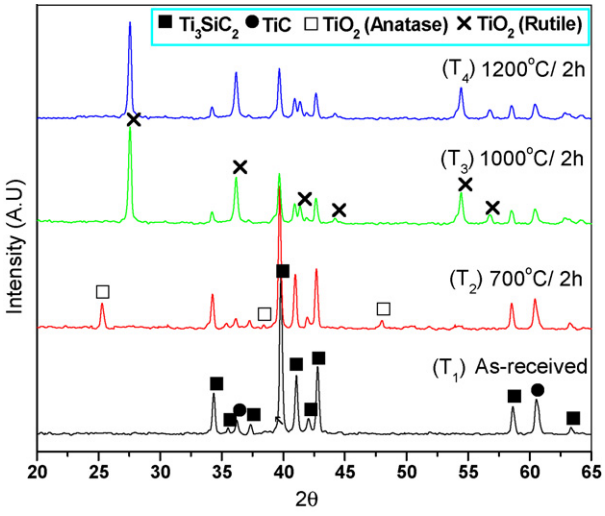

Fig. 4 – XRD analysis represents the different phase of as-received and oxidized specimens. With formation of oxide phase, minute peak shifting could be observed for Ti_3SiC_2 phase (1 0 4), which is represented as ↖ mark.

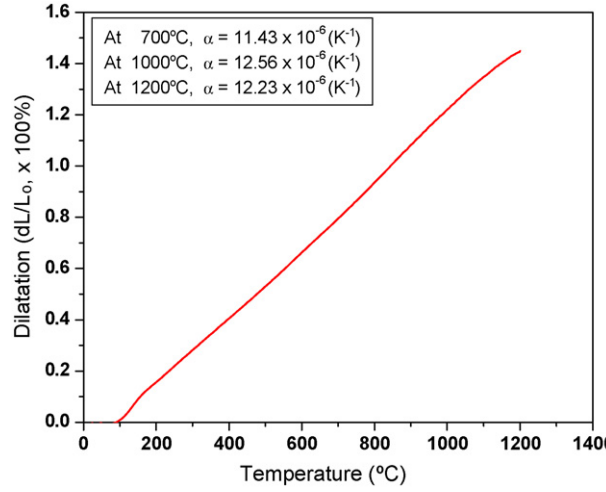

Fig. 5 – Dilatometric curve of Ti_3SiC_2 at heating rate of 5 °C min^{-1}, where CTE increases up to 1000 °C.

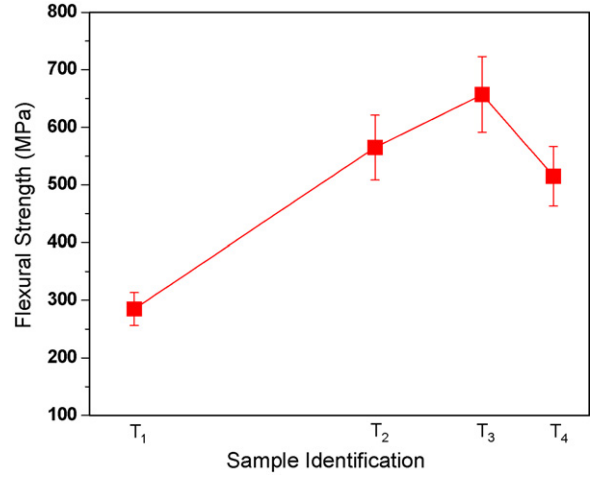

Fig. 6 – Room temperature 3-pt flexural strength of as-received and after heat-treated specimens at corresponding peak temperature for 2 h.

of the oxide scale for the sample oxidized at 1200 °C for 2 h, where the oxygen content of inner surface is higher than that of the outer region (Fig. 2(a) and (b)). The outer 60 m oxide layer is predominately composed of Ti and O. The elemental analysis suggests the inner layer is probably composed of TiO_2 and SiO_2 (thickness ~100 μm). The SiO_2 in the inner layer may be cristobalite phase as suggested by Racault et al. (1994) during oxidation of Ti_3SiC_2. Fig. 3 reveals the variation of oxide scale thickness at different temperatures. Two layers are formed (an inner and outer layer) with different thickness during oxidation from 700 to 1200 °C for 2 h. The thickness of oxide strata varies from ~75 to 160 μm with respect to temperature. XRD analysis of T_2 exhibits the presence of anatase (Fig. 4). After heat treatment at 700 °C for 2 h, the peak ($2\theta = 39.28$) shifting of the T_1 specimen arises due to the development of residual compressive stresses. The transformation of anatase to rutile phase (~60 vol.%) is observed when temperature reaches to 1000 °C. The continuous oxidation characteristic implies that the oxidation at 1200 °C for 2 h may become rate-controlled

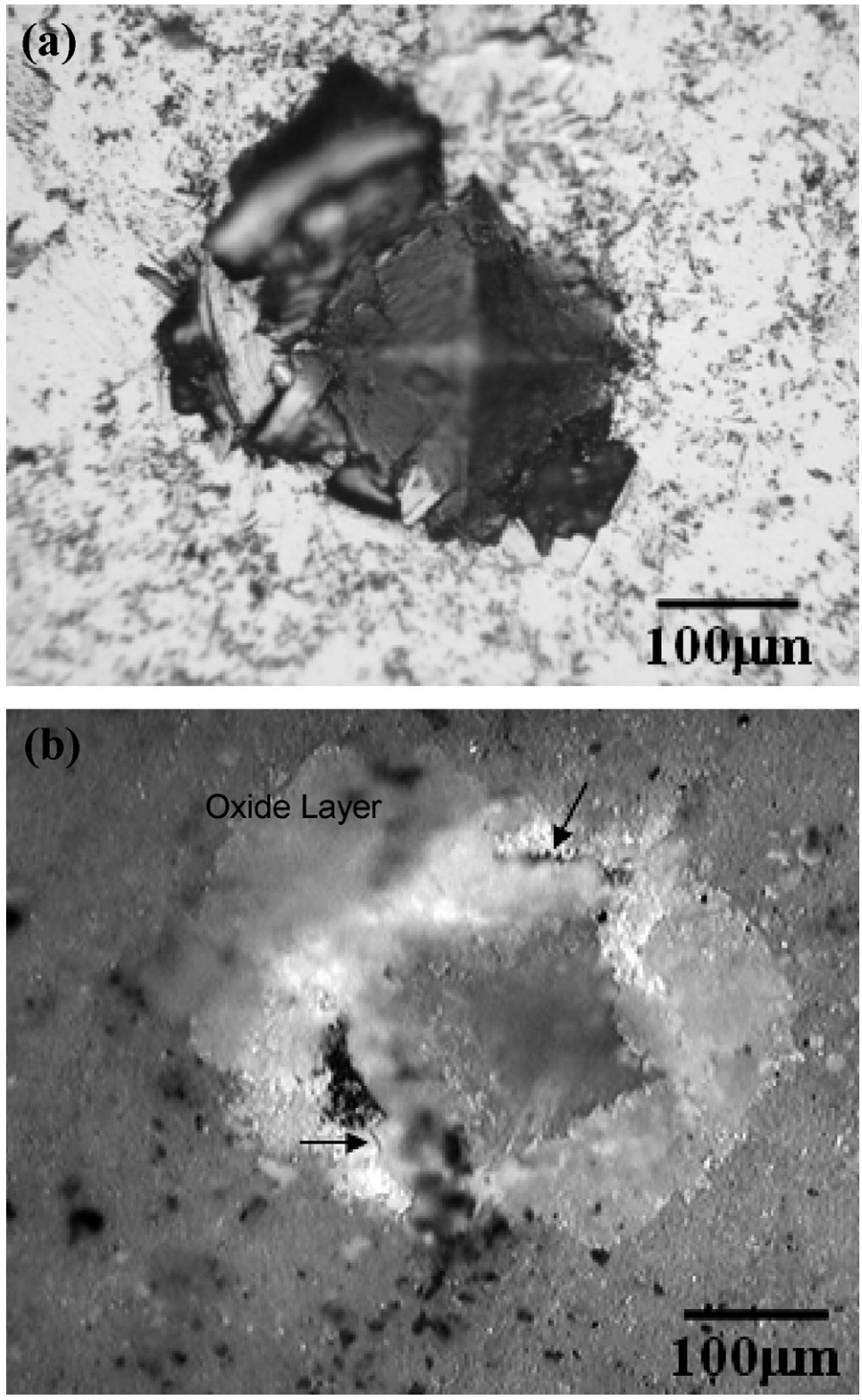

Fig. 7 – SEM image of Vickers indented (98 N) on T_1 (a) and T_4 (b). Original Ti_3SiC_2 surface experiences common grain buckling as well as absence of any radial crack from the indentation edge. A continuous but porous oxide layer and fine microcrack could be visualized in T_4. Different contrast of SEM image illustrates the presence of thick oxide layer.

by the interface reactions. At high temperature, pores are present in the inner TiO_2 and SiO_2 layer and microcracks may be introduced in the outer TiO_2 layer. Consequently, the diffusion-controlled oxidation occurs through the openings of cracks and pores; and subsequent formation of oxide phases. The tendency for the formation of cracks and pores at 1200 °C for 2 h may be raised due to the residual thermal stress resulting from the CTE mismatch of SiO_2 ($12.3 \times 10^{-6}\,K^{-1}$) and TiO_2 ($0.73 \times 10^{-6}\,K^{-1}$) and thicker oxide layers. Barsoum and El-Raghy (1996) revealed that there is no existence of oxidation protection film as SiO_2 on Ti_3SiC_2, however, the oxide scales mainly comprised of an external layer as rutile and an internal layer of rutile and silica. In general, residual stress in the coating or oxidized surface might vary with thickness and temperature (Bao et al., 2007). The dilatation curve of Ti_3SiC_2 specimen is shown in Fig. 5. According to the definition of the coefficient of thermal expansion (CTE) α: $(dL/L_0) = \alpha \times \Delta T$, the value of the slope in Fig. 5, CTE varies in between 11.43 and $12.56 \times 10^{-6}\,K^{-1}$, which is higher than the reported value ($8.5 \times 10^{-6}\,K^{-1}$) in the literature (Manoun et al., in press). At 1000 °C, highest level of compressive residual stress may be attributed due to the development of maximum thermal mismatch within substrate and oxide layer. Fig. 6 illustrates the flexural strength increases up to 650 MPa for heat treatment at 1000 °C for 2 h, however, a sharp fall could be measured beyond this oxidation temperature. At 98 N load, no radial crack is observed around the Vickers indented zone of Ti_3SiC_2 surface, whereas a continuous (different contrast from Ti_3SiC_2 phase) hard TiO_2 layer increases the hardness up to 5.8 GPa (Fig. 7). By microscopic observation of the grains subject to Vickers indentations, the slip or shear deformation could be visualized between the lamellae. Furthermore, the indentation produces considerable material deformation around the indentation zone. This type of indentation behavior was previously reported by Pampuch et al. (1989). In another work, delaminations, deformation of individual grains, grain pull out have been observed in the area of indentations (El-Raghy et al., 1999).

The oxide formation and subsequent increase of flexural strength up to 1000 °C could be observed, however, the strength dramatically reduces at 1200 °C. The strength of oxidized Ti_3SiC_2 specimen is influenced by two components; residual compressive stress due to the formation of oxide phase and strength due to the oxide thickness (Sarkar et al., 2005). The calculated residual stress of T_3 and strength of oxide phase are ~876 and ~173 MPa, respectively (Bao et al., 2007; Sarkar et al., 2007a,b). However, experimental result reveals 657 ± 50 MPa, which is lower due to porous structure of oxide surface. The heterogeneous oxide scale increases at 1200 °C and brittle-to-ductile transition mechanism is predominant which reduces the bending strength (Radovic et al., 2000). It is believed that the main reason for this behavior is the ability of the atomic vibration (phonon) with greater frequency and amplitude with temperature. This increased vibration allows the atoms under stress to slip to new places in the material (i.e. breaking of bonds and formation of new bonds with other atoms in the material). This slippage of atoms is seen on the outside of the material as plastic deformation, which is a common feature of ductile material.

4. Conclusions

At 1200 °C, the oxide layer is mostly comprised of rutile, whereas inner layer is mixture of TiO_2 and SiO_2. A slight peak (1 0 4) shifting of oxidize Ti_3SiC_2 phase could be observed, which is attributed due to the residual compressive stress. Highest CTE is measured at 1000 °C and resultant residual stress has significant effect on strengthening mechanism. Vickers hardness of oxidize specimen has also been slightly increased.

Acknowledgements

This work has been supported in part by a grant (code #: 06K1501-00612) from 'Center for Nanostructured Materials Technology' under '21st Century Frontier R&D Programs' of the Ministry of Science and Technology, Korea.

REFERENCES

Bao, Y.W., Zhou, Y.C., Bu, X.X., Qiu, Y., 2007. Evaluating elastic modulus and strength of hard coatings by relative method. Mater. Sci. Eng. A, doi:10.1016/j.msea.2006.12. 131.

Barsoum, M.W., El-Raghy, T., 1996. Synthesis and characterization of a remarkable ceramic: Ti_3SiC_2. J. Am. Ceram. Soc. 79 (7), 1953–1956.

Casas, B., Ramis, X., Anglada, M., Salla, J.M., Llanes, L., 2001. Oxidation-induced strength degradation of WC-Co hardmetals. Int. J. Refract. Metal Hard Mater. 19, 303–309.

Chu, M.C., Cho, S.J., Yoon, K.J., Park, H.M., 2005. Crack repairing in alumina by penetrating glass. J. Am. Ceram. Soc. 88 (2), 491–493.

Chu, M.C., Cho, S.J., Sarkar, D., Basu, B., Yoon, G.J., Park, H.M., 2006. Oxidation-induced strengthening in ground SiC. J. Mater. Sci. 41 (15), 4978–4980.

Chu, M.C., Panigrahi, B.B., Balakkrishnan, A., Cho, S.J., Yoon, K.J., Kim, T.N., Lee, K.H., in press. Strengthening of alumina by a low thermal expansion glass at surface. Mater. Sci. Eng. A.

El-Raghy, T., Barsoum, M.W., Zavaliangos, A., Kalidindi, S., 1999. Processing and mechanical properties of Ti_3SiC_2. Part II. Mechanical properties. J. Am. Ceram. Soc. 82, 2855–2859.

Manoun, B., Saxena, S.K., Liermann, H.P., Barsoum, M.W., in press. Thermal expansion of polycrystalline Ti_3SiC_2 in the 25–1400 °C temperature range. J. Am. Ceram. Soc. 88 (12), 3489–3491.

Oo, Z., Low, I.M., O'Connor, B.H., in press. Dynamic study of the thermal stability of impure Ti_3SiC_2 in argon and air by neutron diffraction. Physica B.

Pampuch, R., Lis, J., Stobierski, L., Tymkiewicz, M., 1989. Solid combustion synthesis of Ti_3SiC_2. J. Eur. Ceram. Soc. 5, 283.

Racault, C., Langlais, F., Naslain, R., 1994. Solid-state synthesis and characterization of the ternary phase Ti_3SiC_2. J. Mater. Sci. 29, 3384.

Radovic, M., Barsoum, M.W., El-Raghy, T., Seidensticker, J., Wiederhorn, S., 2000. Tensile properties of Ti_3SiC_2 in the 25–1300 °C temperature range. Acta Mater. 48, 453–459.

Rudnik, T., Lis, J., 1997. The Ti_3SiC_2-based structural ceramics. Arch. Metall. 42, 59.
Sarkar, D., Cho, S.J., Chu, M.C., Hwang, S.S., Park, S.W., Basu, B., 2005. Tribological properties of Ti_3SiC_2. J. Am. Ceram. Soc. 88 (11), 3245–3248.
Sarkar, D., Basu, B., Chu, M.J., Cho, S.J., 2006. R-Curve behavior of Ti_3SiC_2, Ceram. Int., Available online 18 April 2006, doi:10.1016/j.ceramint.2006.01.002.
Sarkar, D., Manoj Kumar, B.V., Basu, B., 2006b. Understanding the fretting damage of Ti_3SiC_2. J. Eur. Ceram. Soc. 26 (13), 2441–2452.
Sarkar, D., Basu, B., Chu, M.C., Cho, S.J., 2007a. Is glass infiltration beneficial to improve fretting wear properties for alumina? J. Am. Ceram. Soc. 90 (2), 523–532.
Sarkar, D., Adak, S., Cho, S.J., Chu, M.C., Mitra, N.K., 2007b. Influence of ZrO_2 content and grain size on the thermo-mechanical properties of nano-ZTA. Ceram. Int. 33 (2), 255–261.
Zhang, Z.F., Sun, Z.M., 2005. Shear fracture behavior of Ti_3SiC_2 induced by compression at temperatures below 1000 °C. Mater. Sci. Eng. A 408, 64–71.